JACS
JOURNAL OF THE AMERICAN CHEMICAL SOCIETY
pubs.acs.org/JACS
Article

A Low-Volatile and Durable Deep Eutectic Electrolyte for High-Performance Lithium−Oxygen Battery

Chao-Le Li,[§] Gang Huang,[§] Yue Yu, Qi Xiong, Jun-Min Yan, and Xin-bo Zhang*

Cite This: https://doi.org/10.1021/jacs.1c11711
Read Online

ABSTRACT: The lithium−oxygen battery (LOB) with a high theoretical energy density (~3500 Wh kg^{-1}) has been regarded as a strong competitor for next-generation energy storage systems. However, its performance is still far from satisfactory due to the lack of stable electrolyte that can simultaneously withstand the strong oxidizing environment during battery operation, evaporation by the semiopen feature, and high reactivity of lithium metal anode. Here, we have developed a deep eutectic electrolyte (DEE) that can fulfill all the requirements to enable the long-term operation of LOBs by just simply mixing solid *N*-methylacetamide (NMA) and lithium bis-(trifluoromethanesulfonyl)imide (LiTFSI) at a certain ratio. The unique interaction of the polar groups in the NMA with the cations and anions in the LiTFSI enables DEE formation, and this NMA-based DEE possesses high ionic conductivity, good thermal, chemical, and electrochemical stability, and good compatibility with the lithium metal anode. As a result, the LOBs with the NMA-based DEE present a high discharge capacity (8647 mAh g^{-1}), excellent rate performance, and superb cycling lifetime (280 cycles). The introduction of DEE into LOBs will inject new vitality into the design of electrolytes and promote the development of high-performance LOBs.

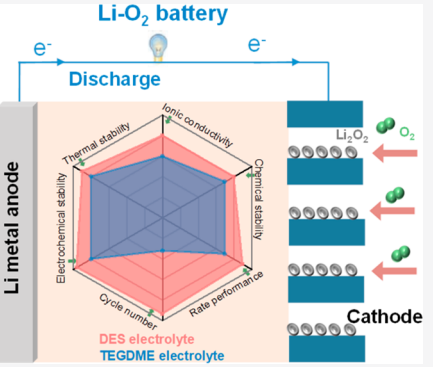

INTRODUCTION

With the rapid development of electronic devices and electric vehicles, traditional lithium-ion batteries (LIBs) have gradually been unable to meet the actual needs of people's daily lives due to their limitations of low achievable energy densities.[1−3] Compared with the available electrochemical energy storage systems, nonaqueous lithium−oxygen batteries (LOBs) with an ultrahigh theoretical energy density of 3500 Wh kg^{-1} have a great possibility to resolve the anxiety of low operation time per battery charge.[4−7] As we know, a long cycling lifetime is one of the prerequisites for realizing the practical application of batteries, while the cycling performance of current LOBs is still far from reaching this level. Among the indispensable components of LOBs, the organic electrolyte plays a crucial role in affecting battery performance.[8−10] However, there are usually serious parasitic reactions between the existing organic electrolytes and the activated oxygen species, like O_2^{2-}, LiO_2, etc., leading to continuous consumption of electrolytes and accumulation of byproducts (e.g., Li_2CO_3 and lithium formate).[11−17] The decomposition of these byproducts requires a high charging voltage, which in turn further induces the decomposition of carbon electrode and electrolyte and eventually causes the battery to fail rapidly with a short lifetime.[18−20] In addition, different from LIB, LOB is a semiopen system, and the organic electrolytes also face the challenge of volatility. This makes it common to use an excess amount of electrolyte that partially dissipates the energy density advantage of LOBs. Nevertheless, even though an electrolyte has low volatility and can endure high charge voltage and attack from active oxygen species, the performance of LOBs may still be unsatisfactory unless the incompatibility issue between the electrolyte and Li metal anode is addressed. Therefore, developing a stable electrolyte with good compatibility to Li metal anode is of great significance to promote the performance improvement of LOBs.

The strong oxidizing environment of LOBs makes the selection of suitable electrolytes a really tough task, and so far, no electrolyte that can fulfill all the above requirements has been designed. Although polar aprotic *N*,*N*-dimethylacetamide (DMA)-based electrolytes are relatively stable to the reactive oxygen species, the intrinsic unstable feature of DMA solvent toward Li metal will cause continuous electrolyte degradation and active Li loss,[21,22] which cannot sustain the long-term running of LOBs. It has been demonstrated that electrolyte regulation, like the change of Li salt or salt concentration, could facilitate the formation of a relatively stable interface between DMA and Li anode to improve the LOB's performance to some extent,[22] but leaves the thermal

Received: November 5, 2021

instability and volatility issues unsolved. To this end, ionic liquid or molten salt-based electrolytes with noninflammability and low vapor pressure would be good choices, and there are already some encouraging results.[23−25] Despite their promise, the high cost of ionic liquids and the high operating temperature of molten salt electrolytes limit their real-world applications. A deep eutectic solvent (DES), which could be prepared by mixing two or more different solid hydrogen bond acceptors and donors at a certain molar ratio, has similar properties to ionic liquids and molten salts.[26] Therefore, designing a deep eutectic electrolyte (DEE) based on DES would not only take over the advantages of ionic liquid/molten salt electrolytes but also get rid of their disadvantages. For example, the interactions of the polar groups in *N*-methylacetamide (NMA) with the cations and anions in Li salt could form room-temperature DEE.[26,27] It should be mentioned that DEEs also have the characteristics of easy preparation, low cost, and being environmentally friendly.[28]

Inspired by the outstanding features of DEEs and the ability of NMA (a kind of amide like DMA) to fight against the attacks from the reactive oxygen species, here, we have developed a new type of NMA-based DEE by just mixing NMA and lithium bis(trifluoromethanesulfonyl)imide (LiTFSI) for LOBs. This NMA-based DEE with good compatibility to Li metal anode and high thermal, chemical, and electrochemical stability well inherits the advantages of amide-based electrolytes and DEEs, overcoming the shortcomings of commonly used organic electrolytes. As a result, the NMA-based DEE enables the stable cycling of LOBs with fewer byproduct formation. Most importantly, the lifetime of LOBs with NMA-based DEE could be further improved at a high temperature of 60 °C, 8 times that of the cell with tetraethylene glycol dimethyl ether (TEGDME)-based electrolyte. The designed stable DEE expands the choice of LOBs' electrolytes.

RESULTS AND DISCUSSION

For preparing NMA-based DEE, the first and most important thing is to choose a suitable Li salt that could easily form DEE with NMA. Considering the delocalization of large anion $TFSI^-$ in LiTFSI, both the cation and anion of LiTFSI would form interactions with the polar groups of NMA to form a DEE, so LiTFSI was selected here.[29,30] As expected, a homogeneous and transparent liquid solution was formed when mixing solid NMA and LiTFSI at a molar ratio of 4:1 (Figure S1). The selection of this molar ratio (4:1) is mainly under the consideration of the eutectic point of the DEE with a molar fraction of lithium salt close to 0.20.[29] Since the formation of the NMA-based DEE is closely related to the interaction of NMA and LiTFSI, Fourier transform infrared spectroscopy (FTIR) analysis was performed. As shown in Figure S2, after mixing with LiTFSI, the amide I C═O in the NMA moves from 1655.3 to 1661.5 cm^{-1}, and the H-bonded N−H I and H-bonded N−H II increase from 3294.6 and 3099.4 cm^{-1} to 3301.4 and 3119.8 cm^{-1}, respectively.[31] The oxygen atom in the C═O group of NMA has a tendency to coordinate with the Li^+ cations, and the H in the NH_2 group of NMA can interact with the anion of LiTFSI, consequently breaking the (N−H···O) hydrogen bond in the NMA and the ionic bond in LiTFSI to form a DEE.[31] The Raman spectra further confirm that the ionic bond in LiTFSI is broken by the interaction between NMA and LiTFSI (Figure S3). The schematic diagram of the interaction between NMA and LiTFSI is shown in Figure 1a. After this, the ionic conductivity of the NMA-based DEE was checked. It is clear that the Li^+ conductivity of NMA-based DEE is always higher than that of TEGDME-based electrolyte (1 M $LiCF_3SO_3$ in TEGDME), and the value is even ∼3 times that of the TEGDME-based electrolyte at 60 °C (3.75 vs 1.27 mS cm^{-1}, Figure 1b). Furthermore, the NMA-based DEE also has a comparable Li^+ transference number to that of TEGDME-based electrolyte (0.60 vs 0.61, Figure S4). Besides ionic conductivity, thermal, chemical, and electrochemical stability is also an important indicator to value the properties of electrolyte. Unlike the serious weight loss of TEGDME-based electrolyte from 100 °C, there is only a small weight change for the NMA-based electrolyte before 150 °C (Figure 1c), revealing its low volatility and high thermal stability and thus the ability to support the long-term operation of semiopen LOBs at high temperatures. For electrochemical stability, the linear sweep voltammetry (LSV) curves show that the NMA-based DEE exhibits a much smaller decomposition current than the TEGDME-based electrolyte from 2.0 to 5.0 V (Figure 1d), demonstrating the NMA-based DEE could withstand the high voltage induced degradation.

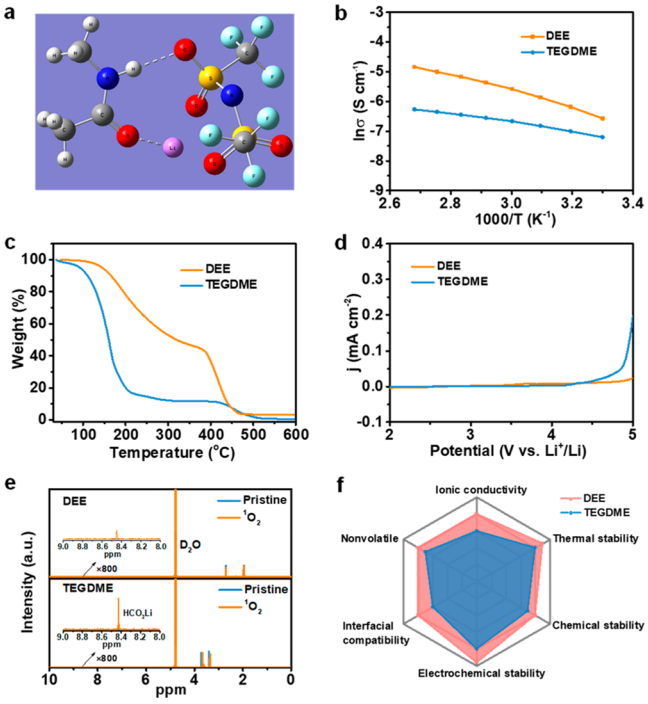

Figure 1. (a) Schematic representation of the interaction between NMA and LiTFSI. (b) Ionic conductivity at different temperatures, (c) thermogravimetric analysis (TGA) curves, and (d) LSV curves of the TEGDME- and NMA-based electrolytes. (e) ^1H NMR spectra of TEGDME- and NMA-based electrolytes before and after treatment with $^1O_2$. (f) Radar plots of the characteristics for TEGDME- and NMA-based electrolytes.

Next, the chemical stability of the electrolyte with the presence of reactive oxygen species was measured. Singlet oxygen ($NaClO/H_2O_2$) was added to NMA- or TEGDME-based electrolyte and then analyzed by nuclear magnetic resonance (NMR) spectroscopy. It can be seen that there are substantial amounts of lithium formate (8.44 ppm, Figure 1e) and lithium acetate (1.89 ppm, Figure S5) byproducts in the treated TEGDME-based electrolyte. In contrast, much fewer byproducts are observed in the NMA-based DEE (Figure 1e),

https://doi.org/10.1021/jacs.1c11711
J. Am. Chem. Soc. XXXX, XXX, XXX−XXX

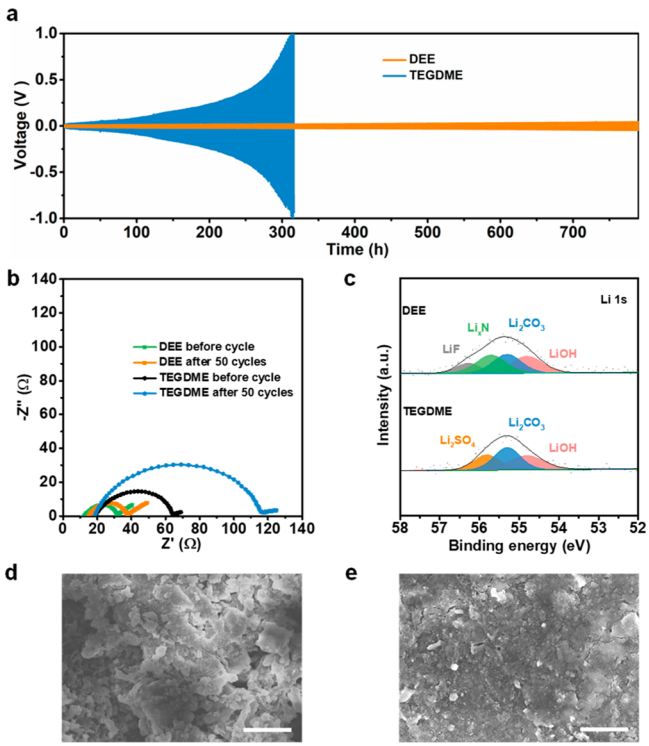

Figure 2. (a) Galvanostatic cycling performance of the Li/Li symmetrical cells with different electrolytes at a current density of 0.1 mA cm^{-2}. (b) Nyquist plots of the Li/Li symmetrical cells before and after cycling for 50 cycles. (c) Li 1s XPS spectra of the Li metal electrodes with different electrolytes after cycling. SEM images of the Li metal electrodes with (d) TEGDME- and (e) NMA-based electrolytes after cycling for 50 cycles. Scale bar, 10 μm.

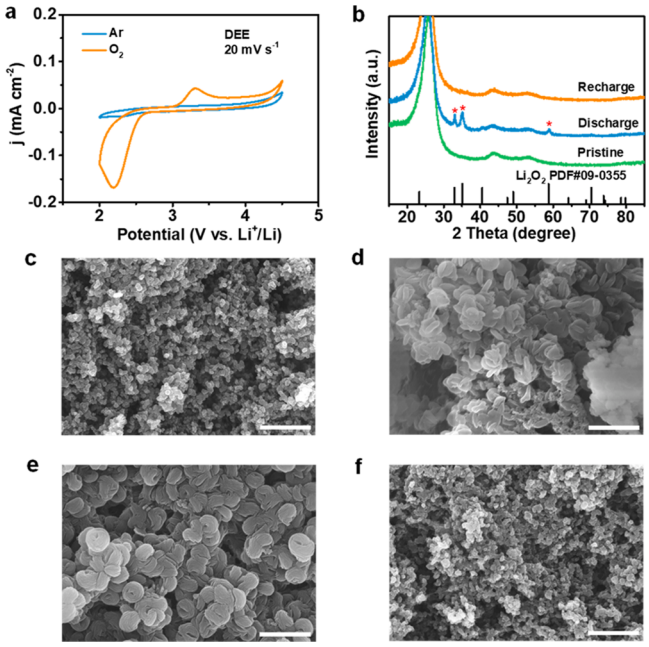

Figure 3. (a) CV curves of the glassy carbon working electrode in NMA-based electrolyte under Ar and O_2 atmosphere. (b) XRD patterns of the pristine, discharged, and recharged Super P cathodes in NMA-based electrolyte. SEM images of the Super P cathodes (c) before discharge and after discharge in (d) TEGDME- and (e) NMA-based electrolytes and (f) recharged in NMA-based electrolyte. Scale bar, 1 μm.

confirming its strong chemical stability. This can be further demonstrated by the FTIR analysis. After mixing with the reactive oxygen species, the infrared peaks corresponding to NMA-based DEE experience no obvious change without detected formation of side reaction products (Figure S6).

Then we moved to investigate the compatibility of the Li metal anode in the NMA-based DEE by checking the cycling performance of Li/Li symmetrical battery at 0.1 mA cm^{-2} in an oxygen environment. As shown in Figure 2a, the Li/Li symmetrical battery with NMA-based DEE exhibits low overpotential and long cycling stability (more than 790 h), which is much better than the battery with TEGDME-based electrolyte that could only cycle 316 h. The long cycling stability of the battery with NMA-based DEE is probably due to the formation of a stable Li/electrolyte interface. To confirm this, electrochemical impedance spectroscopy (EIS) of the Li/Li symmetrical batteries before and after cycling was measured. It is clear that the interfacial impedance of the battery with NMA-based DEE is much smaller than the one with TEGDME-based electrolyte at both the initial and cycled states, and the battery with NMA-based DEE displays a much slower increasing trend for interfacial impedance (Figure 2b), revealing that the NMA-based DEE could facilitate the formation of a stable Li/electrolyte interface. The significant impedance increase of the battery with TEGDME-based electrolyte can be attributed to the severe Li dendrite growth induced generation of a thick solid electrolyte interphase (SEI) layer and dead Li, which is verified by the following scanning electron microscopy (SEM) observation.

X-ray photoelectron spectroscopy (XPS) spectra were subsequently collected to analyze the composition of the SEI film on the cycled Li electrodes (Figure 2c). In Li 1s spectra, two different peaks from Li_xN and LiF appear in the SEI film on the electrode with NMA-based DEE, which originate from the decomposition of NMA and LiTFSI. The existence of Li_xN and LiF can also be observed in the N 1s and F 1s spectra (Figure S7), while for the SEI film on the electrode with TEGDME-based electrolyte, there are no peaks from LiF even with the existence of $LiCF_3SO_3$. In NMA-based DEE, the interactions of the polar groups in the NMA with the cations and anions in the LiTFSI change this situation, and both NMA and $TFSI^-$ could contribute to the construction of SEI film. It has been validated that the Li_xN and LiF are beneficial to stabilizing the Li/electrolyte interface and thus inhibit Li dendrite growth.[32] The SEM image of the Li electrode in TEGDME-based electrolyte manifests irregular Li dendrite growth with large cracks after cycling (Figure 2d). On the contrary, the Li electrode in NMA-based DEE exhibits a flat surface without discernible Li dendrites (Figure 2e), indicating that the stable Li/NMA-based DEE interface could enable uniform Li plating/stripping. As a result, the NMA-based DEE is conducive to the formation of a more stable SEI film than the TEGDME-based electrolyte, overcoming the long-standing conundrum of the incompatibility between Li metal and amide. Then, Li/Cu cells were assembled to test the Coulombic efficiency of different kinds of electrolytes. As shown in Figure S8a,b, the Coulombic efficiency of TEGDME-based electrolyte is only 48.9% in the first cycle and decreases rapidly in subsequent cycles. In addition, another two kinds of common electrolytes (DMA-based and dimethyl sulfoxide-based electrolytes) in Li−O_2 batteries also exhibit low Coulombic efficiencies in Li/Cu cells (Figure S9), while for NMA-based electrolyte, the Coulombic efficiency could reach

https://doi.org/10.1021/jacs.1c11711
J. Am. Chem. Soc. XXXX, XXX, XXX−XXX

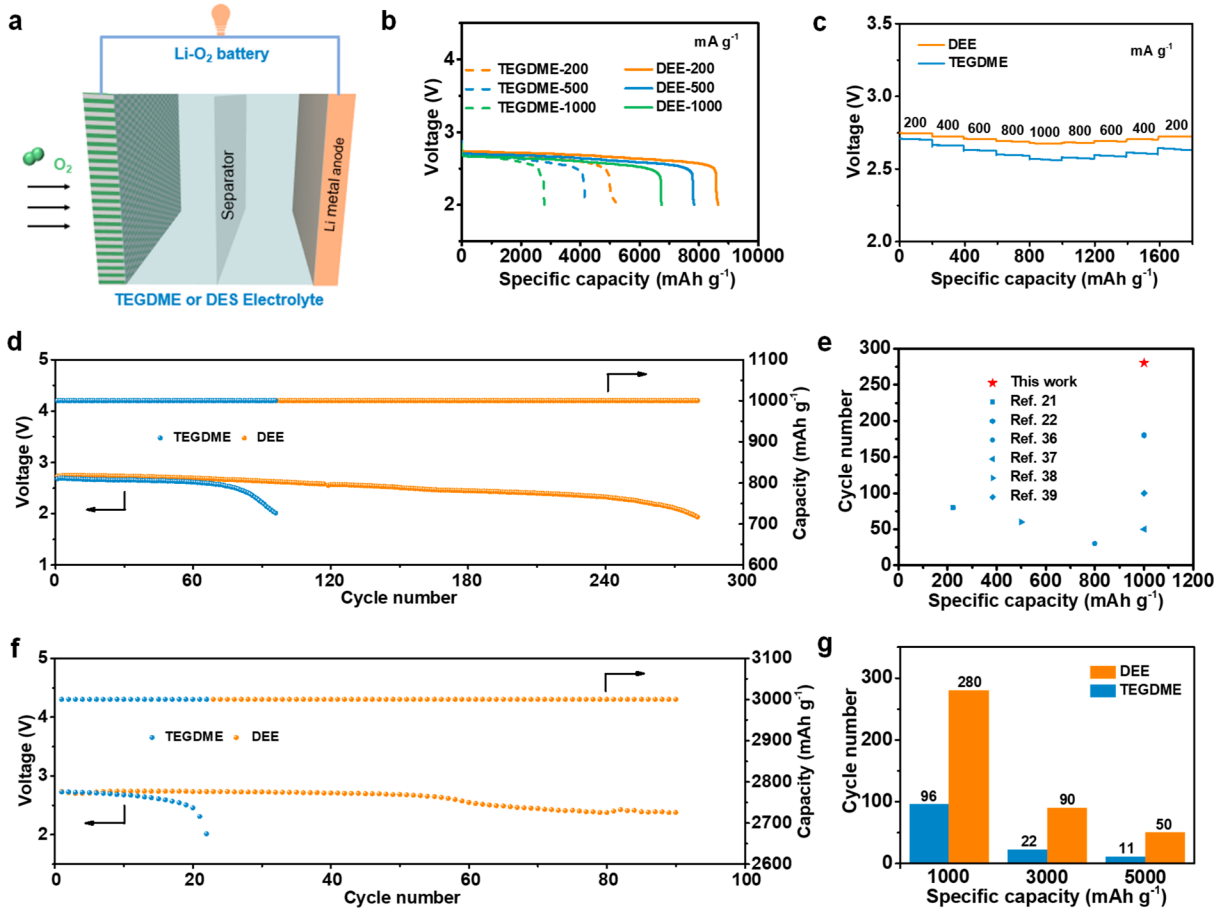

Figure 4. Electrochemical performance of the LOBs. (a) Schematic illustration of a LOB. (b) Full discharge curves at current densities of 200, 500, and 1000 mA g^{-1}. (c) Rate performance at various current densities. Cycle performance with the Ru/CNTs cathodes at limited specific capacities of (d) 1000 and (f) 3000 mAh g^{-1} and a current density of 500 mA g^{-1}. (e) Cycle performance comparison of the LOBs with amide-based electrolytes. (g) Histogram of the cycle life of LOBs at different specific capacities.

58.2% in the first cycle and gradually increases in the following cycles (Figure S8c,d), highlighting the beneficial effects of the NMA-based electrolyte in enabling stable plating and stripping of Li. In sum, the designed NMA-based DEE combines the following advantages together: high ionic conductivity, excellent thermal, electrochemical, and chemical stability, and good compatibility with the Li anode (Figure 1f), which is expected to be a promising electrolyte for LOBs.

To prove the practical applicability of the NMA-based DEE in LOB, cyclic voltammetry (CV) measurement was first conducted in Ar or O_2 atmosphere (Figure 3a). There are no redox peaks when scanned in the Ar environment, suggesting that the electrolyte does not involve any redox reactions. Changing the Ar working atmosphere to O_2 makes the emergence of reduction and oxidation peaks at approximately 2.2 and 3.3 V, which is similar to that of the cell with TEGDME-based electrolyte (Figure S10). This indicates that the NMA-based DEE permits the LOB to follow the typical Li−O_2 electrochemistry reaction. Then, the discharge products on the Super P cathode were characterized by discharging and recharging the battery. The X-ray diffraction (XRD) patterns show characteristic Li_2O_2 diffraction peaks for the discharged cathode, which disappear after the following recharge process (Figure 3b). SEM images in Figure 3c−e reveal that the discharge products in the NMA-based DEE grow uniformly and are larger in size, which can be attributed to the high donor number (DN) value of the NMA rendered solution discharge pathway.[33−35] After recharge, the discharge products completely disappear, and the cathode recovers to the original state with clean surfaces (Figure 3f), further uncovering the reversibility of Li_2O_2 formation and decomposition. In addition, Raman spectra also provide strong support for the reversible conversion of O_2 and Li_2O_2 in the NMA-based DEE (Figure S11).

Figure 4a gives a schematic diagram of LOB with different types of electrolytes. Considering that NMA-based DEE could enable the discharge process to follow the solution pathway, we first checked the full discharge performance of LOBs at various current densities with a cutoff voltage of 2.0 V. As shown in Figure 4b, at the selected current densities, the LOBs with NMA-based DEE deliver constantly higher discharge capacities than the batteries with TEGDME-based electrolyte. Even at a large current density of 1000 mA g^{-1}, the LOB with NMA-based DEE could still provide a discharge capacity of 6740 mAh g^{-1}, more than 2 times that of the TEGDME-based LOB delivered (2785 mAh g^{-1}). The rate performance of the LOBs is displayed in Figure 4c. Despite changing the current densities for every 200 mAh g^{-1}, the LOB with NMA-based DEE exhibits higher and more stable discharge voltages when compared to the one with TEGDME-based electrolyte, which proves that the NMA-based DEE could guarantee the LOB with excellent rate performance. Figure S12 depicts the room-

https://doi.org/10.1021/jacs.1c11711
J. Am. Chem. Soc. XXXX, XXX, XXX−XXX

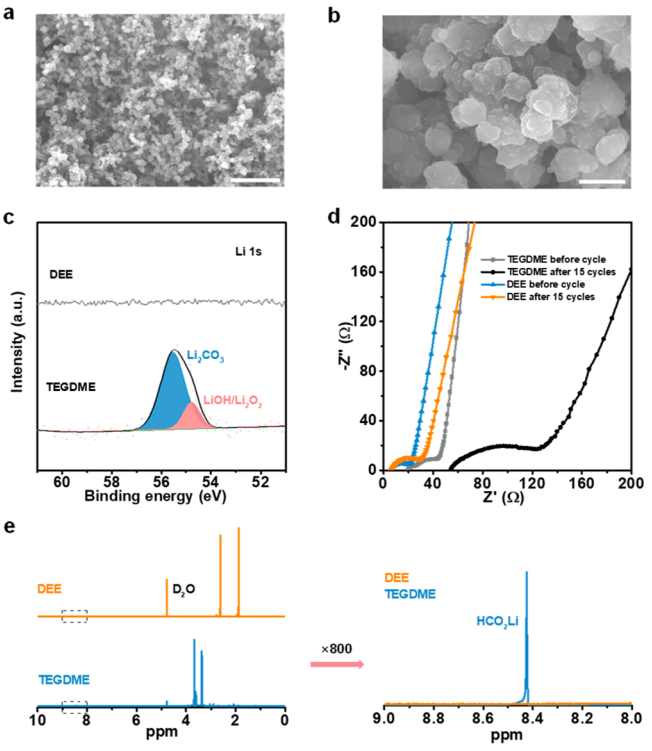

Figure 5. Analysis of the LOBs after 15 cycles. SEM images of the Super P cathodes in (a) NMA- and (b) TEGDME-based electrolytes (scale bar, 1 μm). (c) Li 1s XPS spectra of the cathodes. (d) Nyquist plot of the LOBs. (e) ^{1}H NMR spectra of the TEGDME- and NMA-based electrolytes after cycling.

temperature cycling performance of LOBs. Clearly, the LOB with NMA-based DEE manifests a longer lifetime than the TEGDME-based LOB, but it is still unsatisfactory. The high viscosity of the NMA-based DEE at ambient temperature is the leading cause of this inferior cycling performance. We then increased the testing temperature to 60 °C to reduce the viscosity of NMA-based DEE. As can be seen from Figure S13, the viscosity of NMA-based electrolyte is 18.9 mPa·s at 60 °C, a little bit higher than that of the TEGDME-based electrolyte (3.6 mPa·s). Despite the low viscosity, only 15 cycles are obtained for the TEGDME-based LOB at a current density of 500 mA g^{-1} with a limited specific capacity of 1000 mAh g^{-1} (Figure S14), while for LOB with NMA-based DEE, the cycling performance improves a lot, and the battery can stably operate up to 120 cycles (Figure S15). Additionally, the NMA-based LOB could achieve a lifetime of 70 cycles at a rigorous high temperature of 100 °C (Figure S16). As a contrast, the cycling performance of the LOBs with other commonly used electrolytes was also tested at 60 °C. Both the 1,2-dimethoxyethane (DME, 0 cycle, Figure S17) and DMA (2 cycles, Figure S18) based LOBs nearly cannot work, highlighting the high-temperature resistance of the NMA-based DEE.

When changing the Super P cathode to Ru/CNTs, the cycling life of the NMA-based LOB can be further meliorated and is still much better than that of the TEGDME-based LOB (280 vs 96 cycles, Figure 4d, Figure S19, and Figure S20). Doubling the current density to 1000 mA g^{-1}, the cycling life of the NMA-based LOB just decreases from 280 to 200 cycles (Figure S21). Inspiringly, the performance of the NMA-based LOB achieved here is much superior to those of reported LOBs with amide-based electrolytes (Figure 4e).[36−39] It is worth noting that the loading mass of Ru/CNTs is 0.1 mg cm^{-2} here. To exploit the energy density advantage of LOBs, their high-capacity cycling performance was studied. At a limited capacity of 3000 mAh g^{-1}, the LOB with NMA-based DEE could realize 90 stable cycles, while this value is only 22 cycles for the battery with TEGDME-based electrolyte (Figure 4f). Even further increasing the cycling capacity to 5000 mAh g^{-1}, a lifetime of 50 cycles can still be reached for the NMA-based LOB (Figure 4g, Figure S22). These results reveal that the NMA-based DEE makes the long-term operation of LOBs at high temperatures and large capacities become possible.

To unveil the reasons for the improved electrochemical performance of NMA-based LOB, SEM was first used to analyze the state of the Super P cathodes after 15 cycles (Figure 5a,b). In TEGDME-based LOB, there are still some undecomposed products remaining on the cathode after charging (Figure 5b), whereas the discharge products on the cathode of NMA-based LOB are removed with the recovery of the cathode to the initial state (Figure 5a). This can be further supported by the Li 1s XPS and Raman spectra (Figure 5c and Figure S23). Even after 50 cycles, the cathode surface in the NMA-based LOB keeps clean without any discernible accumulation of byproducts (Figure S24), suggesting the high stability of the NMA-based DEE. In addition, EIS measurement was performed to analyze the impedance change of the LOBs before and after cycling. After 15 cycles, the impedance of the NMA-based LOB only undergoes a slight increase, while both the cell and interfacial impedances of the TEGDME-based LOB increase several times (Figure 5d), which induces the elevation of polarization just as the discharge−charge curves show. The large impedance change for the TEGDME-based LOB can be ascribed to the volatilization and decomposition of electrolyte, the accumulation of byproducts on the cathode, and the unstable electrolyte/anode interface. Furthermore, the electrolytes after cycling were collected and examined by NMR. From Figure 5e, we can see that different from the existence of lithium formate byproducts in the TEGDME-based electrolyte, the NMA-based DEE could remain stable, which is a crucial feature to enable the long-term stable running of LOBs.

In order to further demonstrate the advantages of the NMA-based DEE itself, $LiFePO_4$ was used as a pseudo anode to construct LOBs to eliminate the interference of lithium metal anode. As shown in Figure S25a, the TEGDME-based LOBs could only run 45 cycles at 500 mA g^{-1} and 1000 mAh g^{-1}, while the lifetime of the NMA-based LOBs achieves over 500 cycles by just using the Super P cathode (Figure S25b,c). This big lifetime difference between the two kinds of batteries further illustrates that the main reason for the failure of the TEGDME-based LOBs is the electrolyte itself. Furthermore, the cycling life of the NMA-based LOB can be prolonged to 1000 cycles by changing the Super P cathode with Ru/CNTs (4000 h, Figure S26). This undoubtedly proves that the low-volatile and durable NMA-based DEE could work for a long time in the semiopen and rigorous environment of the LOBs, indicating that it has a great application potential to enable the LOBs to realize an ultralong cycling lifetime.

■ CONCLUSION

In summary, a new-type of NMA-based DEE that can endure the harsh working conditions of LOBs has been designed. The new DEE can not only overcome the disadvantages of the poor

https://doi.org/10.1021/jacs.1c11711
J. Am. Chem. Soc. XXXX, XXX, XXX−XXX

Li anode compatibility of amide-based electrolytes, high cost of ionic liquid, and high operating temperature of molten salt electrolytes but also well retain their advantages, like strong stability toward active oxygen species, low vapor pressure, ability to sustain high temperature, etc. Therefore, the NMA-based DEE facilitates the reversibility of LOBs with fewer byproducts formation, thus realizing satisfactory electrochemical performance, including high discharge capacity, excellent rate capability, and long-term cycling stability. The findings here deepen our understanding of the possibility of applying DEEs to LOBs and provide new opportunities for designing high-performance electrolytes to promote the practical application of LOBs.

■ ASSOCIATED CONTENT

Supporting Information

The Supporting Information is available free of charge at https://pubs.acs.org/doi/10.1021/jacs.1c11711.

Synthesis, FTIR spectra, Raman spectra, NMR spectra, XPS spectra, CV curves, and SEM images of electrolytes or cathodes; physical properties of different electrolytes; electrochemistry performance of LOBs (PDF)

■ AUTHOR INFORMATION

Corresponding Author

Xin-bo Zhang − *State Key Laboratory of Rare Earth Resource Utilization, Changchun Institute of Applied Chemistry, Chinese Academy of Sciences, Changchun 130022, P. R. China;* orcid.org/0000-0002-5806-159X; Email: xbzhang@ciac.ac.cn

Authors

Chao-Le Li − *Key Laboratory of Automobile Materials, Ministry of Education, Department of Materials Science and Engineering, Jilin University, Changchun 130022, P. R. China; State Key Laboratory of Rare Earth Resource Utilization, Changchun Institute of Applied Chemistry, Chinese Academy of Sciences, Changchun 130022, P. R. China*

Gang Huang − *State Key Laboratory of Rare Earth Resource Utilization, Changchun Institute of Applied Chemistry, Chinese Academy of Sciences, Changchun 130022, P. R. China;* orcid.org/0000-0003-2518-8145

Yue Yu − *State Key Laboratory of Rare Earth Resource Utilization, Changchun Institute of Applied Chemistry, Chinese Academy of Sciences, Changchun 130022, P. R. China*

Qi Xiong − *Key Laboratory of Automobile Materials, Ministry of Education, Department of Materials Science and Engineering, Jilin University, Changchun 130022, P. R. China; State Key Laboratory of Rare Earth Resource Utilization, Changchun Institute of Applied Chemistry, Chinese Academy of Sciences, Changchun 130022, P. R. China*

Jun-Min Yan − *Key Laboratory of Automobile Materials, Ministry of Education, Department of Materials Science and Engineering, Jilin University, Changchun 130022, P. R. China;* orcid.org/0000-0001-8511-3810

Complete contact information is available at: https://pubs.acs.org/10.1021/jacs.1c11711

Author Contributions

§C.-L.L. and G.H. contributed equally.

Notes

The authors declare no competing financial interest.

■ ACKNOWLEDGMENTS

This work was financially supported by the National Natural Science Foundation of China (Grant 21725103), National Key R&D Program of China (Grant 2017YFA0206704), Key Research Program of the Chinese Academy of Sciences (Grant ZDRW-CN-2021-3), and K. C. Wong Education Foundation (Grant GJTD-2018-09).

■ REFERENCES

(1) Lu, J.; Li, L.; Park, J. B.; Sun, Y. K.; Wu, F.; Amine, K. Aprotic and aqueous Li-O_2 batteries. *Chem. Rev.* **2014**, *114*, 5611−5640.

(2) Chu, S.; Majumdar, A. Opportunities and challenges for a sustainable energy future. *Nature* **2012**, *488*, 294−303.

(3) Zhang, P.; Zhao, Y.; Zhang, X. Functional and stability orientation synthesis of materials and structures in aprotic Li-O_2 batteries. *Chem. Soc. Rev.* **2018**, *47*, 2921−3004.

(4) Bruce, P. G.; Freunberger, S. A.; Hardwick, L. J.; Tarascon, J. M. Li-O_2 and Li-S batteries with high energy storage. *Nat. Mater.* **2012**, *11*, 19−29.

(5) Ottakam Thotiyl, M. M.; Freunberger, S. A.; Peng, Z.; Chen, Y.; Liu, Z.; Bruce, P. G. A stable cathode for the aprotic Li-O_2 battery. *Nat. Mater.* **2013**, *12*, 1050−1056.

(6) Lu, J.; Lee, Y. J.; Luo, X.; Lau, K. C.; Asadi, M.; Wang, H. H.; Brombosz, S.; Wen, J.; Zhai, D.; Chen, Z.; Miller, D. J.; Jeong, Y. S.; Park, J. B.; Fang, Z. Z.; Kumar, B.; Salehi-Khojin, A.; Sun, Y. K.; Curtiss, L. A.; Amine, K. A lithium-oxygen battery based on lithium superoxide. *Nature* **2016**, *529*, 377−382.

(7) Peng, Z.; Freunberger, S. A.; Chen, Y.; Bruce, P. G. A reversible and higher-rate Li-O_2 battery. *Science* **2012**, *337*, 563−566.

(8) Yao, X.; Dong, Q.; Cheng, Q.; Wang, D. Why Do Lithium-Oxygen Batteries Fail: Parasitic Chemical Reactions and Their Synergistic Effect. *Angew. Chem., Int. Ed.* **2016**, *55*, 11344−11353.

(9) Luntz, A. C.; McCloskey, B. D. Nonaqueous Li-air batteries: a status report. *Chem. Rev.* **2014**, *114*, 11721−11750.

(10) Feng, N.; He, P.; Zhou, H. Critical Challenges in Rechargeable Aprotic Li-O_2 Batteries. *Adv. Energy Mater.* **2016**, *6*, 1502303.

(11) Bryantsev, V. S.; Giordani, V.; Walker, W.; Blanco, M.; Zecevic, S.; Sasaki, K.; Uddin, J.; Addison, D.; Chase, G. V. Predicting solvent stability in aprotic electrolyte Li-air batteries: nucleophilic substitution by the superoxide anion radical ($O_2^{\bullet-}$)). *J. Phys. Chem. A* **2011**, *115*, 12399−12409.

(12) Laino, T.; Curioni, A. A new piece in the puzzle of lithium/air batteries: computational study on the chemical stability of propylene carbonate in the presence of lithium peroxide. *Chemistry* **2012**, *18*, 3510−3520.

(13) Mizuno, F.; Nakanishi, S.; Kotani, Y.; Yokoishi, S.; Iba, H. Rechargeable Li-Air Batteries with Carbonate-Based Liquid Electrolytes. *Electrochemistry* **2010**, *78*, 403−405.

(14) Freunberger, S. A.; Chen, Y.; Peng, Z.; Griffin, J. M.; Hardwick, L. J.; Barde, F.; Novak, P.; Bruce, P. G. Reactions in the rechargeable lithium-O_2 battery with alkyl carbonate electrolytes. *J. Am. Chem. Soc.* **2011**, *133*, 8040−8047.

(15) Gao, X.; Chen, Y.; Johnson, L.; Bruce, P. G. Promoting solution phase discharge in Li-O_2 batteries containing weakly solvating electrolyte solutions. *Nat. Mater.* **2016**, *15*, 882−888.

(16) Peng, Z.; Freunberger, S. A.; Hardwick, L. J.; Chen, Y.; Giordani, V.; Barde, F.; Novak, P.; Graham, D.; Tarascon, J. M.; Bruce, P. G. Oxygen reactions in a non-aqueous Li^+ electrolyte. *Angew. Chem., Int. Ed.* **2011**, *50*, 6351−6355.

(17) Zhang, X.; Guo, L.; Gan, L.; Zhang, Y.; Wang, J.; Johnson, L. R.; Bruce, P. G.; Peng, Z. LiO_2: Cryosynthesis and Chemical/Electrochemical Reactivities. *J. Phys. Chem. Lett.* **2017**, *8*, 2334−2338.

(18) Freunberger, S. A.; Chen, Y.; Drewett, N. E.; Hardwick, L. J.; Barde, F.; Bruce, P. G. The lithium-oxygen battery with ether-based electrolytes. *Angew. Chem., Int. Ed.* **2011**, *50*, 8609−8613.
(19) Ottakam Thotiyl, M. M.; Freunberger, S. A.; Peng, Z.; Bruce, P. G. The carbon electrode in nonaqueous Li-O_2 cells. *J. Am. Chem. Soc.* **2013**, *135*, 494−500.
(20) Zhou, B.; Guo, L.; Zhang, Y.; Wang, J.; Ma, L.; Zhang, W. H.; Fu, Z.; Peng, Z. A High-Performance Li-O_2 Battery with a Strongly Solvating Hexamethylphosphoramide Electrolyte and a LiPON-Protected Lithium Anode. *Adv. Mater.* **2017**, *29*, 1701568.
(21) Walker, W.; Giordani, V.; Uddin, J.; Bryantsev, V. S.; Chase, G. V.; Addison, D. A rechargeable Li-O_2 battery using a lithium nitrate/N,N-dimethylacetamide electrolyte. *J. Am. Chem. Soc.* **2013**, *135*, 2076−2079.
(22) Yu, Y.; Huang, G.; Du, J.-Y.; Wang, J.-Z.; Wang, Y.; Wu, Z.-J.; Zhang, X.-B. A renaissance of N,N-dimethylacetamide-based electrolytes to promote the cycling stability of Li-O_2 batteries. *Energy Environ. Sci.* **2020**, *13*, 3075−3081.
(23) Giordani, V.; Tozier, D.; Tan, H.; Burke, C. M.; Gallant, B. M.; Uddin, J.; Greer, J. R.; McCloskey, B. D.; Chase, G. V.; Addison, D. A Molten Salt Lithium-Oxygen Battery. *J. Am. Chem. Soc.* **2016**, *138*, 2656−2663.
(24) Xia, C.; Kwok, C. Y.; Nazar, L. F. A high-energy-density lithium-oxygen battery based on a reversible four-electron conversion to lithium oxide. *Science* **2018**, *361*, 777−781.
(25) Karkera, G.; Prakash, A. S. An Inorganic Electrolyte Li-O_2 Battery with High Rate and Improved Performance. *ACS Appl. Energy Mater.* **2018**, *1*, 1381−1388.
(26) Hansen, B. B.; Spittle, S.; Chen, B.; Poe, D.; Zhang, Y.; Klein, J. M.; Horton, A.; Adhikari, L.; Zelovich, T.; Doherty, B. W.; Gurkan, B.; Maginn, E. J.; Ragauskas, A.; Dadmun, M.; Zawodzinski, T. A.; Baker, G. A.; Tuckerman, M. E.; Savinell, R. F.; Sangoro, J. R. Deep Eutectic Solvents: A Review of Fundamentals and Applications. *Chem. Rev.* **2021**, *121*, 1232−1285.
(27) Boisset, A.; Jacquemin, J.; Anouti, M. Physical properties of a new Deep Eutectic Solvent based on lithium bis[(trifluoromethyl)-sulfonyl]imide and N-methylacetamide as superionic suitable electrolyte for lithium ion batteries and electric double layer capacitors. *Electrochim. Acta* **2013**, *102*, 120−126.
(28) Wu, J.; Liang, Q.; Yu, X.; Lü, Q. F.; Ma, L.; Qin, X.; Chen, G.; Li, B. Deep Eutectic Solvents for Boosting Electrochemical Energy Storage and Conversion: A Review and Perspective. *Adv. Funct. Mater.* **2021**, *31*, 2011102.
(29) Boisset, A.; Menne, S.; Jacquemin, J.; Balducci, A.; Anouti, M. Deep eutectic solvents based on N-methylacetamide and a lithium salt as suitable electrolytes for lithium-ion batteries. *Phys. Chem. Chem. Phys.* **2013**, *15*, 20054−20063.
(30) Liu, W.; Yi, C.; Li, L.; Liu, S.; Gui, Q.; Ba, D.; Li, Y.; Peng, D.; Liu, J. Designing Polymer-in-Salt Electrolyte and Fully Infiltrated 3D Electrode for Integrated Solid-State Lithium Batteries. *Angew. Chem., Int. Ed.* **2021**, *60*, 12931−12940.
(31) Chen, Y.; Yu, D.; Fu, L.; Wang, M.; Feng, D.; Yang, Y.; Xue, X.; Wang, J.; Mu, T. The dynamic evaporation process of the deep eutectic solvent $LiTf_2N$:N-methylacetamide at ambient temperature. *Phys. Chem. Chem. Phys.* **2019**, *21*, 11810−11821.
(32) Wang, Q.; Yao, Z.; Zhao, C.; Verhallen, T.; Tabor, D. P.; Liu, M.; Ooms, F.; Kang, F.; Aspuru-Guzik, A.; Hu, Y. S.; Wagemaker, M.; Li, B. Interface chemistry of an amide electrolyte for highly reversible lithium metal batteries. *Nat. Commun.* **2020**, *11*, 4188.
(33) Lai, J.; Xing, Y.; Chen, N.; Li, L.; Wu, F.; Chen, R. Electrolytes for Rechargeable Lithium-Air Batteries. *Angew. Chem., Int. Ed.* **2020**, *59*, 2974−2997.
(34) Johnson, L.; Li, C.; Liu, Z.; Chen, Y.; Freunberger, S. A.; Ashok, P. C.; Praveen, B. B.; Dholakia, K.; Tarascon, J. M.; Bruce, P. G. The role of LiO_2 solubility in O_2 reduction in aprotic solvents and its consequences for Li-O_2 batteries. *Nat. Chem.* **2014**, *6*, 1091−1099.
(35) Xu, J. J.; Chang, Z. W.; Wang, Y.; Liu, D. P.; Zhang, Y.; Zhang, X. B. Cathode Surface-Induced, Solvation-Mediated, Micrometer-Sized Li_2O_2 Cycling for Li-O_2 Batteries. *Adv. Mater.* **2016**, *28*, 9620−9628.
(36) Choudhury, S.; Wan, C. T.; Al Sadat, W. I.; Tu, Z.; Lau, S.; Zachman, M. J.; Kourkoutis, L. F.; Archer, L. A. Designer interphases for the lithium-oxygen electrochemical cell. *Sci. Adv.* **2017**, *3*, e1602809.
(37) Kim, Y.; Koo, D.; Ha, S.; Jung, S. C.; Yim, T.; Kim, H.; Oh, S. K.; Kim, D. M.; Choi, A.; Kang, Y.; Ryu, K. H.; Jang, M.; Han, Y. K.; Oh, S. M.; Lee, K. T. Two-Dimensional Phosphorene-Derived Protective Layers on a Lithium Metal Anode for Lithium-Oxygen Batteries. *ACS Nano* **2018**, *12*, 4419−4430.
(38) Lim, H.-D.; Yun, Y. S.; Ko, Y.; Bae, Y.; Song, M. Y.; Yoon, H. J.; Kang, K.; Jin, H.-J. Three-dimensionally branched carbon nanowebs as air-cathode for redox-mediated Li-O_2 batteries. *Carbon* **2017**, *118*, 114−119.
(39) Yoo, E.; Zhou, H. LiF Protective Layer on a Li Anode: Toward Improving the Performance of Li-O_2 Batteries with a Redox Mediator. *ACS Appl. Mater. Interfaces* **2020**, *12*, 18490−18495.

https://doi.org/10.1021/jacs.1c11711
J. Am. Chem. Soc. XXXX, XXX, XXX−XXX